Measurement and Calculation of Absolute Rotational Strengths for Camphor, α-Pinene, and Borneol

Petr Bouř,*,† Jennifer McCann, and Hal Wieser

Department of Chemistry, University of Calgary, 2500 University Drive, Calgary, AB T2N 1N4, Canada

Received: May 20, 1997; In Final Form: October 17, 1997[⊗]

Experimental dipole and rotational strengths of the three optically active terpenes were compared to those obtained from the magnetic field perturbation (MFP) and vibronic coupling theory (VCT), and the results were analyzed in order to facilitate future extension of current vibrational circular dichroism (VCD) simulation techniques to bigger molecules. Experimental VCD patterns could be faithfully reproduced by both calculations, but the absolute VCD intensities are usually underestimated. The size of the basis set is the main limitation in both the MFP and VCT calculations. Harmonic frequencies and dipolar strengths obtained by Hartree−Fock and five density functional methods are compared to experiment for α-pinene. For borneol, a natural occurrence and spectral representation of its conformers are discussed on the basis of comparison of the theoretical and experimental frequencies and VCD and absorption intensities.

Introduction

The technique of vibrational circular dichroism (VCD) can now be routinely used for studies of molecular structure of small and medium-sized molecules[1−3] as well as for biopolymers.[4] The interpretation of the spectra is almost entirely dependent on ab initio calculations of transition frequencies and intensities. Given the limits of the computations, more approximations have to be used for bigger molecules, and often a limit is reached when theoretical predictions become unreliable. It is generally accepted that calculated spectral intensities require a much larger basis set than force fields if a similar level of accuracy should be achieved. Often, however, a limited accuracy of simulated intensities is sufficient for spectral analyses, if it enables an unambiguous assignment of observed transitions. This is a situation commonly encountered in the VCD spectroscopy because the sign of VCD signal enhances the assignment. In this study we want to investigate the limitations of such an approach based on a quantitative comparison of theoretical results with experimental intensities.

Because of their strong VCD signal and low price, terpenes are widely used for calibrating vibrational optical activity measurements. Simulated and experimental band shapes are routinely compared to test calculational procedures.[5,6] However, VCD and absorption spectra are rarely analyzed in terms of absolute intensities of individual transitions. This information is difficult to obtain especially for the VCD spectra, due to their lower signal-to-noise (S/N) ratio. Also, band overlapping and band cancellation can lead to an almost unpredictable error for these intensities. Occasionally an anharmonic interaction or solvent shift can lead to a misinterpretation of observed values. Nevertheless, we find it useful to compare the experimental values to theory and determine to what degree a simple comparison of the spectral shapes is justified. Although the computations are performed for a molecule in vacuum, we experienced that a nonpolar solvent does not change the intensity pattern by more than few percent on average.

We compare the two most widely used ab initio theories of VCD, namely the vibronic coupling theory[7] (VCT), implemented as a complementary program to Gaussian 90 program package, and the magnetic field perturbation theory (MFP),[8,9] implemented in the Cadpac set of programs.[10] The difference between the two approaches is in the treatment of the electronic part of the atomic axial tensors (AAT) defined as

$$I^{\lambda}_{\alpha\beta} = \langle \partial n/\partial R^{\lambda}_{\alpha} | \partial n/\partial B_{\beta} \rangle \qquad (1)$$

where $\partial n/\partial R^{\lambda}_{\alpha}$ is the derivative of the electronic ground-state wave function, $|n\rangle$, with respect to an α-coordinate of an atom λ, and $\partial n/\partial B_{\beta}$ is the derivative with respect to a β-component of an external magnetic field. While MFP theory uses (1) directly, the VCT theory is based on an alternate expression

$$I^{\lambda}_{\alpha\beta} = \sum_j W_{jn}^{-1} \langle \partial n/\partial R^{\lambda}_{\alpha} | j \rangle \langle j | m_{\beta} | n \rangle \qquad (2)$$

which can be straightforwardly derived from the former by the insertion of the sum over the excited states, $1 = \sum_j |j\rangle\langle j|$, and taking advantage of elementary properties of the magnetic dipole moment operator $\mathbf{m}$.[11] $W_{jn} = W_j - W_n$ is the electronic excitation energy. If implemented on the Hartree−Fock (HF) level, VCT and MFP are believed to yield results of similar quality when the origin dependence of calculations with incomplete bases is removed using a distributed origin gauge transformation or the magnetic field dependent atomic orbitals. The performance of the two approaches was tested previously on small systems.[12] Here we are interested in the comparison for relatively large molecules, where a lower level of approximation must be used. Exploration of the behavior of such lower-level calculations is important for future calculations on even larger systems, like peptides and nucleic acid segments. As shown below, the ultimate limit of the accuracy of such VCD computations is given by the size of the basis set of the atomic orbitals rather than by the theoretical scheme used for the calculation.

* Corresponding author.

† Permanent address: Institute of Organic Chemistry and Biochemistry, Academy of Sciences of the Czech Republic, Flemingovo nam 2, 16610, Praha 6, Czech Republic.

⊗ Abstract published in *Advance ACS Abstracts,* December 1, 1997.

S1089-5639(97)01665-4 CCC: $15.00
Published on Web 01/01/1998

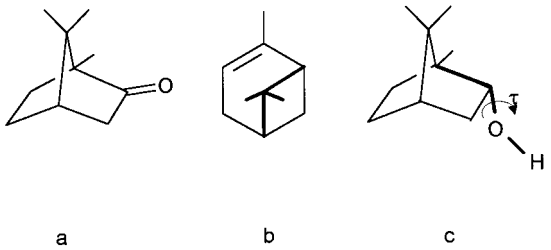

Figure 1. (1*R*)-(−)-Camphor (a), (−)-α-pinene (b), and [(1*R*)-*endo*]-(−)-borneol (c).

Modern hybrid HF-density functional theory (DFT) functionals found numerous applications in quantum chemistry, although no general rules exist that would enable one to decide beforehand which particular functional should be used for a special task. To test the qualities of harmonic force fields obtained by most common functionals, we compare the frequencies for α-pinene to those obtained by experiment. For this molecule, vibrational transitions are relatively well-resolved and recently we assigned spectral bands for the Raman and Raman optical activity spectra.[13]

From the point of view of the potential of VCD as a means for studying conformational changes in molecules, we find it interesting also to analyze the VCD spectrum of *endo*-borneol. This molecule is a well-defined model system with limited conformational freedom, expressed exclusively by the rotation of the OH group. As shown later, this rotation has a profound influence on the resultant VCD pattern, which can be modeled with the ab initio calculations. Thus, an actual conformation or conformational equilibrium can be determined, albeit with limited accuracy, by the VCD technique when other experimental tools can be used only with difficulties (like NMR) or cannot be used at all (X-ray spectroscopy).

Experimental Section

The description of our VCD spectrometer can be found elsewhere.[14] The available spectral range with this instrument is approximately 800−1700 cm^{-1}, determined by the ZnSe photoelastic modulator and detector sensitivity. The spectra of the compounds were measured for solutions in CCl_4 (0.36 M for camphor, 0.40 M for borneol). Trial measurements (not reported here) in CS_2 lead to almost the same values for vibrational frequencies and intensities, but with a lower S/N ratio. The chemicals were purchased from Aldrich and used without further purification. NaCl cells were used with an optical path length of 0.15 mm. A total of 500 dc and 5000 ac scans were accumulated for the VCD measurements with a resolution of 4 cm^{-1}. The experimental VCD spectra were corrected for baseline deviations by subtracting the VCD spectrum of the opposite enantiomer for (1*S*)-(−)-camphor and (1*S*)-(−)-α-pinene, and by subtracting the VCD spectrum of the solvent for ([(1*S*)-*endo*]-(−)-borneol (Figure 1). The reliability of the experimental VCD spectrum is evaluated from the noise estimate, which is displayed at the zero VCD baseline. The noise estimate was calculated by adding either the VCD spectra of the two opposite enantiomers (corrected by the racemic compounds) or two consecutive spectral scans, divided by 2, for Figures 2 and 4, respectively.

Calculation

The geometry of the molecules was optimized by an energy minimization using the Becke3LYP (B3L) DFT functional[15,16] with the 6-31G** basis set. For borneol, the three conformers were calculated separately with both Becke3LYP/6-31G** and HF/6-31G** methods. For the minimized geometries, harmonic force fields were calculated at the same level of approximation. The program Gaussian 94[17] was used for the calculation.

Recently, ionization energies and other electronic properties obtained by various hybrid HF-DFT functionals were compared.[18] From the perspective of vibrational spectroscopy, we found it useful to test the quality of the harmonic force field provided by the most common functionals as defined in the Gaussian program. Thus force fields of α-pinene were calculated for optimized geometries with the 6-31G** basis set for the HF approximation, the local (spin) density approximation (LDA), Becke's three-parameter functional and Perdew's 1991 expression for the correlation[19] (B3P), Becke's 1988[20] exchange and Perdew's 1991 correlation functional (BPW), Becke's three-parameter functional combined with Perdew's 1986 correlation (P86),[21] and finally, the B3L functional.

The local parts of the atomic axial tensors were calculated at the HF level. Programs Cadpac 5.0[10] and VCT90[7] were used for MFP and VCT calculations, respectively. Then the axial tensors were combined with the Becke3LYP/6-31G** atomic polar tensors (using the distributed origin gauge) and harmonic force field to produce the spectral intensities. Frequencies were uniformly scaled by a factor of 0.9752 for camphor and borneol to facilitate the comparison of calculated spectra with the experimental data. VCD and absorption spectra were simulated using Lorentzian band shapes with a uniform half-width of 5 cm^{-1}.

Experimental VCD and absorption spectra were analyzed using the Labcalc software.[22] Baseline-adjusted mixed Lorentzian−Gaussian bands were fitted to observed bands. VCD and absorption peaks were fit independently. The peak positions of the resolved absorption bands were taken as the observed transition frequencies. The dipole (*D*) and rotational (*R*) strengths were calculated from the integrated areas using the relations

$$D = 9.184 \times 10^{-3} \int \epsilon \, (\mathrm{d}\nu/\nu) \tag{3}$$

$$R = 2.296 \times 10^{-3} \int \Delta\epsilon (\mathrm{d}\nu/\nu) \tag{4}$$

where ϵ and $\Delta\epsilon$ are the absorption and VCD intensity, respectively, in L mol^{-1} cm^{-1}. The strengths *D* and *R* are in units of (debye)^2 (1 debye (D) = 10^{-18} esu cm = 3.33546 × 10^{-30} C m).

The experimental frequencies, dipole strengths, and rotational strengths were compared with the calculated values using a linear regression $X_{CAL} = aX_{EXP}$. The coefficient "*a*" was determined by a least-squares fit and the standard deviations ($\delta = [\sum_{i=1,N}(X_{CAL,i} - aX_{EXP,i})^2/N)]^{1/2}$, *N* the number of transitions) were calculated.

Results and Discussion

Spectra of Camphor. In Table 1 the calculated harmonic frequencies, dipole strengths, and rotational strengths are compared with the accessible experimental values for the camphor molecule. The experimental VCD intensity of the C═O stretching mode could not be measured because of the high absorption and a low anisotropic ratio for this band. The rotational strength R_{APT} in Table 1 was calculated using the APT model, i.e., the local magnetic contributions to AAT were neglected.[23] A detailed description of the normal mode displacements in terms of potential energy distributions was not determined since observed transitions can be unambiguously

TABLE 1: Comparison of Calculated and Experimental VCD and Absorption Intensities and Frequencies for (1*R*)-(−)-Camphor[a]

mode	ω_{cal}	ω_{exp}	D_{cal}	D_{exp}	R_{APT}	R_{MFP}	R_{MFP}*	$R_{MFP}m$	R_{VCT}	R_{exp}
75	3062		36		29	57	58		40	
74	3050		35		−65	−39	−51		−68	
73	3045		22		−37	−48	−38		−31	
72	3040		45		265	398	439		396	
71	3039		45		−260	−585	−626		−502	
70	3030		51		−380	−838	−925		−568	
69	3030		23		394	837	924		567	
68	3024		4		−2	2	2		11	
67	3021		6		60	243	264		186	
66	3015		42		11	41	31		22	
65	2995		38		−100	−219	−229		−184	
64	2991		17		37	28	37		28	
63	2986		35		32	57	57		44	
62	2973		49		110	111	110		102	
61	2970		24		−96	−147	−148		−140	
60	2966		17		4	13	13		2	
59	1795	1747	452		8	−171	−147	−123	−132	
58	1504	1480	11	13	28	20	14	29	21	−3
57	1492	1470	11	16	−85	−96	−83	−114	−93	−200
56	1488		1		−6	−10	−10	−16	−9	”
55	1476		8	23	39	5	3	8	16	
54	1472	1454	7	”	−32	−60	−44	−60	−51	−102
53	1467	1448	11	42	−34	−52	−33	−40	−44	46
52	1462		13	”	12	12	5	15	12	”
51	1458		6		24	13	0	11	15	”
50	1434	1417	25	28	11	8	8	23	6	50
49	1404	1390	20	26	32	48	46	55	46	96
48	1388	1376	12	13	6	−20	−21	−28	−15	−50
47	1383	1372	13	20	5	10	9	17	10	20
46	1320	1324	17	22	49	−73	−71	−107	−69	−149
45	1305	1278	3	6	20	27	19	48	25	152
44	1299	1294	6	3	7	5	23	50	10	
43	1273	1276	23	23	−9	16	32	2	15	37
42	1245	1246	10	3	−38	−97	−128	−143	−89	−419
41	1239	1234	0	0	−4	−7	−7	−13	−5	
40	1220	1216	10	4	−43	−48	−33	−24	−50	−3
39	1197	1198	18	8	42	99	89	45	85	123
38	1189	1189	2	3	−11	3	−6	30	7	
37	1161	1166	12	9	−10	−71	−100	−68	−57	−222
36	1145	1151	2	2	5	47	51	67	32	121
35	1120	1128	4	8	−15	−68	−68	−50	−52	−64
34	1093	1093	18	21	−1	78	67	39	52	37
33	1073	1079	6	7	−21	133	95	69	75	−19
32	1033	1045	97	104	50	106	133	167	69	715
31	1014	1021	82	40	19	−57	10	62	12	135
30	1007	1010	3	2	20	5	29	−61	16	−97
29	978	985	0	1	−3	8	8	12	6	47
28	941	952	12	12	−9	8	2	46	3	−35
27	937	984	3		48	68	83	52	59	162
26	923	935	7	16	−29	−48	−56	−76	−44	−148
25	920	925	7	5	−36	−121	−141	−153	−98	−356
24	900	912	6	2	21	86	93	128	68	165
23	849	862	3	8	16	49	56		37	66
22	837	854	6		6	112	102		73	216
21	817	825	2		2	15	11		11	
20	737		35		−22	−229	−224		−158	
19	693		3		5	53	57		36	
18	630		11		7	71	71		45	
17	599		6		31	230	216		153	
16	557		6		−6	−83	−68		−45	
15	542		14		19	98	101		77	
14	509		35		−22	−47	−54		−38	
13	464		4		6	−24	−18		−9	
12	406		12		−14	−10	−15		−14	
11	385		1		−5	−3	−6		−4	
10	372		8		7	−13	−4		−8	
9	291		24		−14	23	7		0	
8	286		5		3	25	35		20	
7	255		13		4	−19	−19		−4	
6	232		13		−2	−17	−19		−10	
5	218		9		8	−1	3		7	
4	203		3		0	15	17		12	

TABLE 1: (Continued)

mode	ω_{cal}	ω_{exp}	D_{cal}	D_{exp}	R_{APT}	R_{MFP}	R_{MFP}*	$R_{MFP}m$	R_{VCT}	R_{exp}
3	162		3		13	35	44		26	
2	159		2		−5	−12	−15		−8	
1	103		136		12	8	16		8	
a	1.003		0.96		0.10	0.24	0.29	0.34	0.20	
δ	16		9		23	47	39	36	35	

[a] ω_{cal} and ω_{exp}: calculated (B3LYP/6-31G**, scaled by a factor of 0.9752) and experimental frequencies, in cm^{-1}. D_{cal} and D_{exp}: calculated (B3LYP/6-31G**) and experimental dipole strengths, in 10^{-4} D^2. Rotational strengths (in 10^{-9} D^2): R_{APT}, atomic polar tensor model; R_{MFP}, MFP method, HF/6-31G basis for AAT; R_{MFP}*, MFP, HF/6-31G* basis for AAT; $R_{MFP}m$, MFP, HF/6-31G* basis for AAT, MP2 force field, from ref 5; R_{VCT}, VCT method, HF/6-31G basis. Symbols "*a*" and "δ" denote the coefficient and the standard deviation for the fit $X_{CAL} = aX_{EXP}$, respectively.

assigned on the basis of spectral intensities and the information does not materially contribute to the argument.

As seen in Table 1, the scaled frequencies match experiment within a few cm^{-1} in most cases. The relatively high standard deviation ($\delta = 16$ cm^{-1}) arises mainly from the error of higher-frequency modes (modes 51−59), while for the rest of spectrum the agreement with experiment is surprisingly good. Better agreement would be difficult to achieve due to multiple factors: anharmonic effects, inadequacy of the ab initio level and of the limited basis set, and omission of molecular environment in the calculation. The Becke3LYP functional, if used with the 6-31G** basis, is known to lead to frequencies which agree within few percent with experiment,[1−2,24] and our findings are in accordance with this experience.

For the dipolar intensity, calculated values are on average 4% lower than experimental values ($a = 0.96$, see Table 1), which can be considered as a rather remarkable success of the theory. The standard deviation is 9×10^{-4} D^2 and this error can be considered relatively small and appropriate, given the experimental error and the known dependence and great sensitivity of absorption intensities on the quality of the ab initio calculations,[11,25] namely on the basis set completeness. Evidently, the B3LYP functional with the 6-31G** basis set lead to a faithful representation of infrared absorptions in the mid- and low-frequency regions. The results also indirectly confirm the previous findings that the molecular nonpolar environment has a minor effect on spectral intensities.[1,2] Obviously, for molecules where hydrogen bonds are formed, for example, such a good agreement could not be expected unless the interaction with the solvent is included in the theoretical model.

The rotational strengths are at the focus of our interest. Unlike the dipole strengths, calculated rotational strengths are largely underestimated and the standard deviations are relatively high. Even the signs are calculated incorrectly for modes 28, 30, 33, and 53, although the assignment of the overlapping bands is futile. This can be expected, however, since the VCD phenomenon is a second-order effect with respect to the multipole expansion of the molecular electromagnetic field[26] and dependent on the gradient of the electronic wave function. The error of the calculation would perhaps be substantially reduced if a bigger basis set could have been used. We do not expect that a post-HF treatment of the AAT or inclusion of gauge-independent atomic orbitals[27] would lead to substantial improvement of the accuracy at this point, although these effects should be certainly tested in the future. Previously, we have experienced that the 6-31G** basis is inadequate for estimating absolute values of such second-order properties as polarizabilities and susceptibilities.[11] Indeed, the addition of the polarization functions to the basis set lead to an overall increase of VCD intensities (cf. R_{MFP} and R_{MFP}* or $R_{MFP}m$ in Table 1). Unfortunately, further extension of the basis set is not possible with current computer limitations, given by the implementations

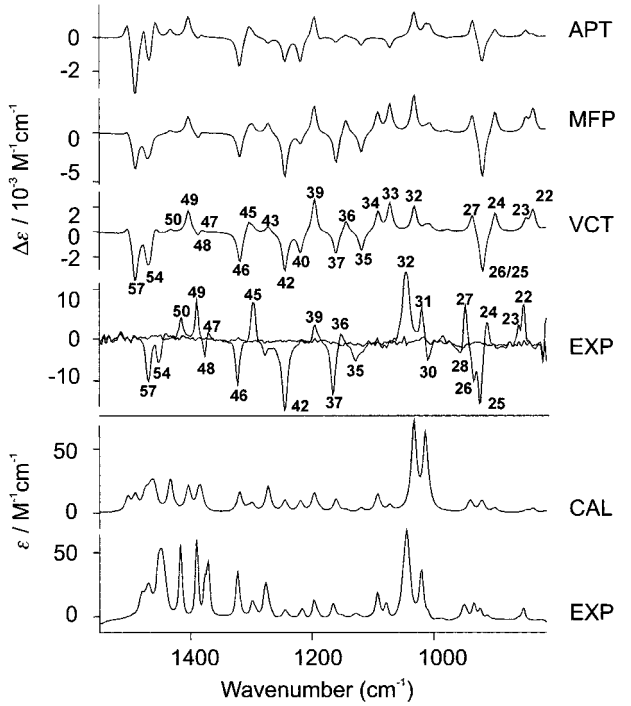

Figure 2. VCD (upper group) and absorption spectra (lower group) of (1*R*)-(−)-camphor. APT, MFP, VCT, and CALC correspond to R_{APT}, R_{MFP}, R_{VCT}, and $D_{calc,}$ respectively, in Table 1. Numbered bands in VCT and EXP VCD spectra correspond to the mode numbers in Table 1. The baseline in the experimental VCD spectrum represents the noise estimate plotted at the same intensity.

of MFP and VCT in Cadpac and VCT90 programs, respectively. Despite these drawbacks, the theoretical modeling still leads to a faithful reproduction of VCD sign patterns and relative intensities for most modes that can be directly compared to the experiment (Figure 2).

The atomic polar tensor model (R_{APT} in Table 1) gives the lowest magnitudes of the rotational strengths. Nevertheless, a majority of the band signs is predicted correctly, and the overall spectral pattern shows a reasonable agreement with experiment. MFP (with the 6-31G basis) lead to slightly higher overall intensities than VCT ($a = 0.24$ for MFP and 0.20 for VCT) but also to a higher standard deviation (δ in Table 1). The rotational strengths $R_{MFP}m$ from ref 5 are based on an MP2 force field and approximate the experiment better ($a = 0.34$) than the corresponding values R_{MFP}* obtained with the DFT force field with $a = 0.29$. However, given the agreement and the uncertainty of the experimental values, the simulation presented here based on the DFT force field can be considered as sufficient.

Comparison of DFT Functionals. In Table 2 we compare the results from the six ab initio approximations with experimental frequencies and dipolar strengths for α-pinene. The

TABLE 2: α-Pinene, Frequencies (ω) and Dipolar Strengths (D) Calculated at Six ab Initio Levels[a]

no.	ω_{HF}	ω_{LDA}	ω_{B3P}	ω_{BPW}	ω_{P86}	ω_{B3L}	ω_{exp}	D_{HF}	D_{LDA}	D_{B3P}	D_{BPW}	D_{P86}	D_{B3L}	D_{EXP}
56	1891	1721	1743	1680	1748	1733	1657	43	28	27	21	27	23	43
55	1656	1453	1526	1489	1525	1533	1485	64	118	111	100	112	89	
54	1649	1447	1517	1479	1517	1526	1469	122	251	142	105	148	102	417
53	1632	1432	1503	1466	1503	1512	1458	4	136	58	86	62	39	
52	1624	1429	1498	1462	1498	1506	1454	72	275	165	137	180	102	
51	1619	1424	1495	1459	1495	1503	1446	75	30	41	33	30	61	751
50	1615	1414	1487	1450	1486	1496	1442	39	33	58	57	56	64	
49	1614	1413	1484	1449	1484	1492	1435	56	300	217	204	222	183	413
48	1607	1403	1481	1442	1480	1490	1417	159	271	89	74	99	48	9
47	1557	1366	1422	1384	1422	1433	1381	88	351	182	140	200	119	185
46	1551	1352	1418	1379	1419	1426	1374	29	476	64	32	75	22	164
45	1542	1344	1406	1365	1406	1415	1364	147	570	271	213	288	163	300
44	1500	1333	1375	1332	1376	1375	1335	70	44	51	49	53	48	53
43	1495	1321	1366	1321	1368	1365	1328	32	47	62	49	57	45	105
42	1470	1301	1345	1301	1346	1345	1305	4	22	18	47	18	35	11
41	1437	1269	1308	1261	1310	1304	1264	24	101	87	87	87	59	123
40	1399	1241	1280	1240	1280	1282	1248	7	14	5	6	6	5	4
39	1390	1229	1257	1213	1258	1256	1220	72	8	118	175	110	119	113
38	1350	1211	1250	1208	1253	1243	1215	177	125	48	55	41	105	46
37	1342	1205	1239	1199	1240	1237	1204	1	52	125	129	124	95	155
36	1324	1174	1213	1174	1214	1214	1181	73	5	68	72	58	84	74
35	1294	1162	1197	1161	1198	1195	1165	6	155	64	87	71	44	85
34	1251	1122	1155	1121	1157	1154	1125	74	44	141	168	133	169	154
33	1240	1087	1133	1095	1134	1133	1100	149	103	89	89	86	75	121
32	1207	1081	1112	1079	1113	1111	1084	107	40	72	86	64	95	127
31	1180	1054	1084	1053	1084	1085	1062	34	96	73	88	77	54	52
30	1160	1041	1070	1037	1071	1068	1042	16	58	51	40	51	39	41
29	1138	1019	1062	1031	1062	1061	1032	58	90	38	46	38	54	46
28	1124	999	1036	1007	1037	1039	1014	97	417	238	236	238	172	176
27	1108	985	1022	994	1022	1026	995	22	11	18	16	17	16	17
26	1061	959	980	950	983	977	959	119	227	146	147	158	168	65
25	1054	942	972	942	972	974	952	58	97	69	65	62	10	173
24	1027	935	955	928	957	956	939	16	95	28	16	34	11	13
23	1014	923	952	923	953	944	927	43	60	32	31	29	34	108
22	996	916	928	899	930	922	905	51	38	13	21	12	30	35
21	971	884	908	878	909	901	886	169	133	153	128	152	121	269
20	928	863	868	838	869	854	842	19	25	31	29	28	31	15
19	900	823	836	806	838	828	821	379	12	4	18	4	11	
18	893	784	810	782	810	812	788	213	102	553	503	542	474	
17	841	776	788	762	790	781	772	59	645	161	190	170	139	
16	722	676	678	657	680	674	666	1	21	4	6	5	2	
15	676	613	625	605	626	625	619	32	39	34	32	32	28	
14	623	560	574	555	575	574	563	71	59	69	66	67	59	
13	519	477	486	473	487	487	480	43	52	48	51	49	47	
12	499	456	465	452	467	467	462	11	40	29	31	28	22	
11	464	415	424	412	424	428	442	67	95	90	93	86	74	
10	425	379	393	382	393	396	394	26	98	39	35	37	30	
9	421	371	388	377	387	390	384	3	7	10	13	10	8	
8	364	321	330	319	329	331	332	114	274	179	185	182	157	
7	327	297	305	297	305	305	302	84	109	119	140	118	118	
6	279	261	261	253	262	262		7	16	14	20	13	13	
5	244	226	230	224	229	229		27	30	32	31	31	25	
4	214	205	203	198	204	204		25	69	52	61	53	49	
3	207	194	194	191	195	194		9	59	18	22	18	14	
2	185	188	188	185	187	186		11	3	8	4	10	7	
1	138	119	129	127	128	129		222	344	270	266	271	223	
a	1.12	0.994	1.12	0.999	1.030	1.031		0.53	1.24	2.6	0.74	0.80	0.60	
δ	15	15	61	9.9	9.6	11.0		54	120	99	49	47	47	

[a] C−H region omitted. Dipolar strengths in 10^{-5} D^2, ω in cm^{-1}. All calculations done with 6-31G** basis set: HF - Hartree−Fock; LDA - local spin density approximation; B3P, BPW, P86, and B3L - the Becke3P86, Becke3PW91, Perdew 86, and Becke3LYP hybrid DFT-HF functionals, respectively. Symbols "*a*" and "d" same as in Table 1. [b] Frequencies 53 and 7−19 obtained from ROA spectra, ref 13.

C−H stretching region is omitted, because the high-frequency region is not accessible for our VCD measurement. Also, the double-harmonic approximation used throughout this work may not be appropriate for the higher-frequency vibrations. As can be seen in the table, the HF calculation overestimates the frequencies by 12% on average ($a = 1.12$), although the standard deviation (15 cm^{-1}) is reasonably small and suggests that a uniform scaling would be justified for this force field. However, dipolar strengths are largely underestimated by the HF calculation ($a = 0.53$) and large deviations from the experimental values for several transitions indicate that the mode ordering is not correctly reproduced (cf. modes 48 and 49, 38 and 39, 25 and 26). In contrast to HF, the LDA calculation underestimates vibrational frequencies and overestimates the dipolar strengths. Although the frequencies are closer to the experiment, the high standard deviation for dipolar strengths ($\delta = 120 \times 10^{-5}$ D^2) suggests severe limitation of LDA for simulation of vibrational spectra. Quite surprisingly, the B3P combination of the DFT

TABLE 3: Calculated and Experimental Rotational Strengths for α-Pinene[a]

no.	R_{VCT}	R_{MFP}	R_{EXP}	no.	R_{VCT}	R_{MFP}	R_{EXP}	no.	R_{VCT}	R_{MFP}	R_{EXP}
56	−5	−3		37	42	71	−35	18	−4	22	
55	19	43		36	−7	−114	−98	17	−36	−53	
54	−12	−2	−38	35	13	32	−54	16	−2	−5	
53	−13	−33		34	−59	−140	−367	15	29	73	
52	8	53	58	33	50	118	380	14	−13	−23	
51	−8	−36	−15	32	19	−15		13	16	52	
50	3	37	−10	31	29	103	148	12	−1	21	
49	3	12		30	20	8	−93	11	4	7	
48	0	−5		29	−6	−43		10	2	−19	
47	17	24	80	28	−89	−190	−232	9	−8	−30	
46	4	−6	30	27	42	146	357	8	21	−21	
45	3	−8		26	39	105	129	7	23	96	
44	3	5	−9	25	−17	−59	−75	6	−11	−17	
43	−26	−61	−153	24	8	26	31	5	−11	−34	
42	−15	−29	−11	23	−27	−30	−66	4	2	6	
41	20	27	156	22	−21	−98	−127	3	−1	7	
40	8	8		21	14	−1	−106	2	−7	−15	
39	−31	128	−45	20	1	−47	−118	1	13	10	
38	31	14	392	19	−12	−39	−32				
a									0.15	0.38	
δ									18	47	

[a] Mode numbers and symbols consistent with Table 2. Rotational strengths in 10^{-9} D^2.

functionals leads to the worst representation of vibrational spectra, overestimating the frequencies by 12% and the dipole strengths by 160%, on average, with huge standard deviations for both cases. These results sharply disagree with the DFT calculations of ionization energies and electron affinities,[18] where all five DFT approaches were found nearly equivalent. From our point of view, only the last three functionals (BPW, P86, and B3L) lead to qualitatively similar results. The BPW calculation led to the best set of harmonic frequencies (a = 0.999!), while the P86 functional provided best dipolar strengths (80% of the experimental values, on average). The B3L calculation overestimated the frequencies by 3% and underestimated the dipolar strengths by 40%. These differences, however, should be considered rather minor, since the true (experimental) harmonic frequencies may differ from the observed transitional frequencies, due to anharmonicities, and the experimental transitions 49−56 could not be resolved. The relative absorption intensities of modes 25 and 26 appear to be given incorrectly by the calculations, whereas the VCD calculation in Table 3 confirms the calculated mode ordering.

VCD of α-Pinene. The rotational strengths are calculated with the B3L force field and listed in Table 3. As for camphor, the VCT calculation leads to smaller average VCD intensities (a = 0.15) than the MFP calculation (a = 0.38), but also to a smaller standard deviation. Many regions in the experimental spectrum could not be resolved completely, which increases the error of the experimental values. For example, the experimental rotational strengths for transitions 54−48 were calculated within a range of only about 40 cm^{-1}, and thus the listed values will probably contain contributions from other modes. Specifically, mode 30 can be mixed with 29 to give the relatively large negative signal observed at 1042 cm^{-1}. Although MFP and VCT give similar quantitative descriptions of the spectrum, more signs predicted by the two methods are opposite for α-pinene (modes 46, 45, 39, 32, 21, and 20) than for camphor (modes 33 and 30) in the mid-IR region. Thus the convergence of both MFP and VCT strengths to a common value should be generally tested for approximate calculations on bigger systems.

Borneol Conformations. Relative energies for the three conformers are given in Table 4, as calculated at the HF/6-31G** and B3LYP/6-31G** levels. The latter calculation was used to estimate the Boltzmann factors and relative populations γ_1 of the three conformations.

TABLE 4: Relative Energies of Borneol Conformers

conformer	τ [deg]	E_{HF}[a]	E_{DFT}[a]	E_{ZP}[a]	γ_1[b]	γ_2[b]
I (gauche −)	−67.8	0	0	0	52	26
II (anti)	−174.7	0.2	1.75	1.49	28	75
III (gauche +)	71.2	3.56	2.37	2.29	20	0

[a] Energies in kJ/mol: HF, HF/6-31G**, DFT, Becke3LYP/6-31G**; and ZP, Becke3LYP/6-31G** zero-point energy. [b] Relative occurrence (%) calculated from a Boltzmann distribution (at 295 K, γ_1) and from the comparison of calculated and experimental spectra absorption intensities (γ_2). The symbol τ is the OH group torsion angle C2−C1−O−H defined in Figure 1, obtained from the DFT calculation.

Calculated and experimental frequencies and dipole strengths for the three conformers are given in Table 5, and corresponding rotational strengths are listed in Table 6. Clearly, the rotation of the OH group causes substantial changes both in absorption and VCD spectra. We attribute such a big influence to the coupling of the C−O stretching and the C−O−H bending modes to the ring deformation modes. As for camphor, the modes are delocalized and cannot be associated with local symmetry coordinates. Although the most profound changes under the influence of conformation can be found in the VCD spectra, where sign inversions can be observed for many bands, it is difficult to extract the intensity information from the experiment for each band separately, since the transitions are overlapped and a conformational equilibrium is likely to take place in the sample. For the absorption spectrum, the calculated dipolar strengths were used to fit the experimental values (using the least-squares fit $D_{exp} = \gamma(\mathrm{I})\ D_{\mathrm{I}} + \gamma(\mathrm{II})_{\mathrm{I}}\ D_{\mathrm{II}} + \gamma(\mathrm{III})\ D_{\mathrm{III}}$, with γ being the molar ratios), which yield the conformer weights γ_2 in Table 4. The spectral intensities suggest that a smaller number of molecules would exist in conformation III than predicted by the Boltzmann factor. Nevertheless, the low VCD signal of this conformer at the higher frequency region may be identified with the experimental pattern. The experimental and calculated spectra are compared in Figure 3 (absorption) and Figure 4 (VCD). The sum corresponds to the relative conformation ratios γ_1 given in Table 4.

Good agreement can be observed between the simulated and experimental absorption spectra in Figure 3. The population

TABLE 5: Frequencies and Dipole Strengths for the Three Borneol Conformers[a]

no.	ω_I	ω_{II}	ω_{III}	ω_{exp}	D_I	D_{II}	D_{III}	D_{exp}
63	1503	1503	1507		8	10	24	
62	1492	1495	1499	1480	17	18	9	22
61	1486	1486	1487	1470	6	3	2	12
60	1482	1482	1483		3	5	6	
59	1474	1475	1478		14	6	11	
58	1474	1473	1475	1453	15	22	19	90
57	1470	1470	1470		11	6	6	
56	1462	1462	1464		3	3	6	
55	1458	1458	1460		0	0	0	
54	1403	1404	1411	1408	14	13	103	11
53	1396	1393	1400	1386	11	8	10	27
52	1385	1385	1386	1372	13	9	12	8
51	1380	1381	1381	1367	14	14	20	20
50	1341	1336	1328	1340	32	33	7	12
49	1312	1311	1312	1305	8	2	1	17
48	1305	1305	1303		0	5	1	
47	1286	1291	1284	1297	30	22	9	4
46	1280	1280	1270		0	2	5	
45	1253	1253	1263	1278	1	3	14	11
44	1237	1242	1242	1249	3	50	1	14
43	1234	1230	1228	1232	134	22	33	29
42	1216	1215	1222	1217	80	9	9	11
41	1203	1196	1195	1197	35	6	7	13
40	1195	1184	1188		4	52	0	
39	1164	1167	1156	1162	4	6	20	7
38	1142	1141	1140	1147	7	6	13	5
37	1130	1130	1116	1132	8	39	21	15
36	1108	1100	1099	1104	38	97	278	52
35	1082	1081	1079	1079	15	30	55	8
34	1057	1060	1061	1054	124	143	171	141
33	1029	1028	1024	1029	30	75	8	38
32	1000	1008	1005	988	119	24	6	16
31	987	985	989	977	11	18	19	13
30	963	964	965	963	18	15	20	
29	938	939	939	956	9	0	6	
28	937	934	936	947	16	15	8	12
27	930	931	929	937	15	42	2	5
26	923	925	923	931	18	15	8	18
25	907	907	905	915	2	2	10	2
24	875	870	867	879	3	1	17	5
23	826	826	821	827	12	7	9	26
22	821	818	819		1	25	13	
21	758	756	750		13	23	4	
20	728	730	726		3	3	11	
19	635	631	633		7	9	7	
18	580	581	578		12	3	11	
17	566	566	562		2	5	13	
16	513	509	513		16	29	13	
15	483	485	483		3	1	7	
14	447	447	451		82	30	70	
13	423	423	420		10	3	4	
12	379	379	381		14	9	21	
11	348	350	361		28	7	147	
10	327	328	338		185	54	32	
9	312	305	300		983	111	84	
8	296	259	286		342	1295	1076	
7	247	246	246		1	65	0	
6	226	226	226		17	8	0	
5	223	223	221		13	34	1	
4	219	216	216		3	12	4	
3	215	212	213		2	76	40	
2	184	183	182		4	1	21	
1	114	113	111		12	14	43	

[a] Frequencies (B3LYP/6-31G** scaled by a factor of 0.9752) in cm^{-1}, dipole and strengths in 10^{-4} D^2, C−H and O−H stretching modes skipped. The conformers are defined in Table 4.

TABLE 6: Rotational Strengths for the Three (1*R*)-*endo*-(−)-Borneol Conformers[a]

no.	$R_{I,MFP}$	$R_{I,VCT}$	$R_{II,MFP}$	$R_{II,VCT}$	$R_{III,MFP}$	$R_{III,VCT}$	R_{exp}
63	47	44	24	23	4	6	
62	−106	−97	−168	−153	−34	−32	−144
61	−23	−19	−25	−20	−11	−9	
60	−7	−8	18	17	0	1	
59	35	35	24	23	−44	−41	
58	56	50	38	34	10	11	113
57	−38	−32	6	5	−6	−6	
56	20	20	23	23	27	25	
55	−4	−5	0	0	3	3	
54	−22	−18	48	41	−41	−40	
53	68	58	−28	−18	41	35	70
52	−34	−44	−8	−15	−3	−6	−31
51	92	90	−15	−9	33	32	94
50	33	26	18	7	−52	−45	
49	−8	−8	−14	−14	−5	−6	−17
48	−7	−6	22	23	27	24	
47	45	36	48	42	−25	−18	69
46	−4	−4	12	10	7	5	
45	−62	−53	51	45	55	59	−180
44	−56	−46	87	69	−42	−36	−125
43	36	−2	−185	−166	−181	−165	−201
42	186	149	121	111	−42	−39	(+)
41	−78	−70	−61	−55	−29	−25	−276
40	−52	−43	−39	−21	−8	−8	
39	−24	−20	−20	−17	−63	−50	−91
38	−36	−29	−59	−50	−93	−78	−80
37	108	98	101	90	222	201	147
36	−109	−103	−135	−130	−152	−131	−405
35	20	12	−62	−58	−80	−71	−49
34	373	317	314	266	333	293	1220
33	−1	−1	−56	−36	−44	−35	28
32	−174	−146	−80	−62	101	91	−411
31	76	67	−78	−71	−18	−22	51
30	−67	−54	43	34	98	88	−48
29	54	48	14	13	73	65	
28	3	9	57	52	−48	−45	157
27	−97	−81	11	6	19	18	−302
26	−107	−90	43	−29	−65	−60	
25	26	21	20	15	62	53	55
24	32	27	10	9	−27	−22	
23	−92	−73	63	−55	−75	−67	−145
22	−28	−22	140	−116	−79	−63	
21	35	27	28	20	14	10	
20	−12	−9	34	29	−36	−27	
19	5	10	0	0	−22	−19	
18	23	21	10	9	−11	−12	
17	−17	−14	6	5	58	42	
16	30	26	48	42	−38	−36	
15	−8	−8	−14	−15	−4	−7	
14	89	76	−55	−52	90	86	
13	−36	−34	10	8	−2	−2	
12	10	9	−7	−6	5	2	
11	14	5	−14	−13	71	62	
10	−181	−140	−71	−53	51	42	
9	−213	−146	59	44	−9	−7	
8	−146	−109	372	280	273	178	
7	0	0	−3	−7	−3	−3	
6	32	30	−10	−9	−4	−2	
5	18	15	−16	−9	−9	−7	
4	−2	−3	−36	−27	9	6	
3	−10	−7	−84	−72	45	34	
2	2	2	8	7	−1	−2	
1	−23	−22	10	8	24	19	

[a] In 10^{-9} D^2.

of conformer I seems to be overestimated in Table 4 as its absorption signal at about 1230 cm^{-1} is not observed in the experimental spectrum. The relatively low calculated occurrence of conformer III is in accord with observation, since its strong predicted bands for modes 34, 36, and 54 do not dominate the experimental spectrum. The thermodynamic average (based on values γ_1) of the VCD spectra obtained by the VCT calculation, as plotted in Figure 4, also gives a reasonable representation of the observed signal. A significant contribution of conformer III in the sample can almost certainly be ruled

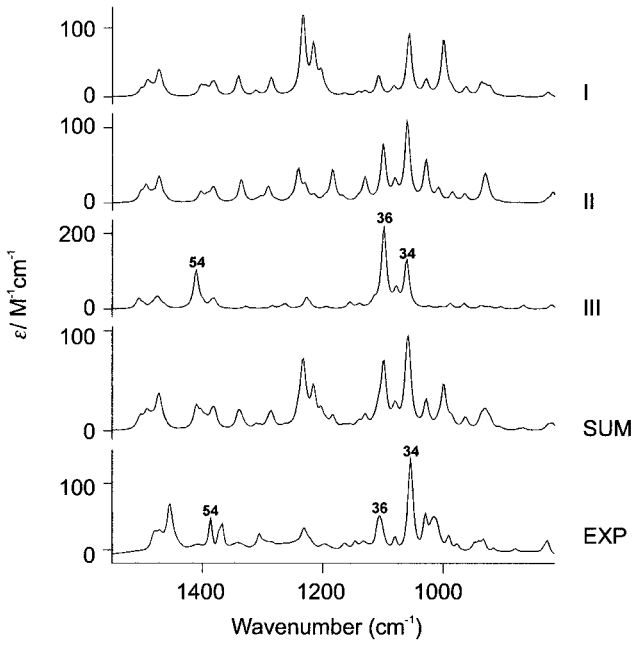

Figure 3. Calculated and experimental absorption spectra of [(1*R*)-*endo*]-(−)-borneol. The symbols I, II, and III refer to the conformers identified in Table 4 and to D_I, D_{II}, and D_{III}, respectively, in Table 5. SUM corresponds to the sum of the three calculated spectra (γ_1 in Table 4).

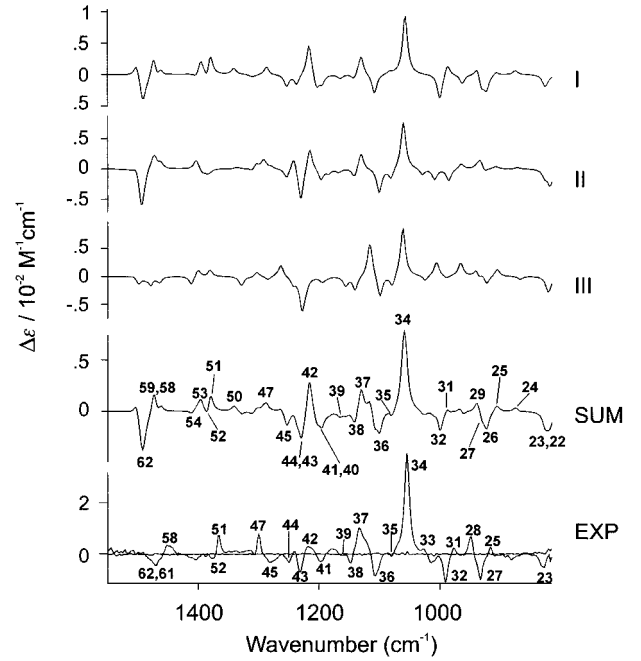

Figure 4. Calculated and experimental VCD spectra of [(1*R*)-*endo*]-(−)-borneol. The symbols I, II, and III refer to the conformers identified in Table 4 and to $R_{I,VCT}$, $R_{II,VCT}$, and $R_{III,VCT}$, respectively, in Table 6. SUM corresponds to the sum of the three calculated spectra (γ_1 in Table 4). Numbered bands in SUM and EXP VCD spectra correspond to the mode numbers in Table 6. The baseline in the experimental VCD spectrum represents the noise estimate plotted at the same intensity.

out, since its simulated spectral features cannot be clearly identified in the experimental VCD. For example, the positive signals predicted for modes 37 and 43 are not apparent in the experimental spectrum. For the values of VCD intensities listed in Table 6, a mixture of conformers I and II explains most of the experimentally observed values, although quantitative conclusions are difficult due to complexities arising from conformational mobility and hydrogen bonding. On the basis of the results for camphor and α-pinene, MFP and VCT theories can be considered nearly equivalent, with perhaps slightly better average performance of MFP. We can demonstrate this with the results for the VCD of the borneol conformers. Clearly, the dependence of the calculated VCD spectrum on the conformation can be modeled quite reliably with either one of the two theoretical approaches. Overall, the analysis of the absorption and VCD spectra is in accordance with the approximate energy estimations given in Table 4. Both the computations of spectral intensities and molecular energies show a limited accuracy. Nevertheless, simulations of VCD and absorption spectra add additional useful information about the actual molecular structure.

Despite the uncertainty of the molar ratios obtained for borneol, the results show the potential of VCD spectroscopy to study molecular conformations. The dramatic dependence of VCD spectra on conformation completes our previous findings for peptides,[3] where we supposed that the VCD signals arise from an interaction of rather isolated chromophores. We found that mechanical coupling between the peptide amide groups is the most important source of peptide optical activity. The results for borneol show the strong effect of mechanical coupling in cyclic systems. This effect should be taken into account when constructing biomolecular force fields[23] where the neglect of coupling can lead to erroneous results.

Conclusions

The high S/N ratio achievable with our instrument enabled us to determine absolute absorption and VCD intensities for most vibrational transitions. While the absorption can be relatively accurately reproduced by the ab initio calculation, both the vibronic coupling and magnetic field perturbation theories for VCD substantially underestimate the dichroic intensities if implemented at the HF level with an incomplete basis set. However, the sign and relative intensity pattern in the VCD spectra can be well-reproduced. Nonpolar solvents cause minor changes in VCD spectra of the terpenes, favoring the direct comparison of experiment with ab initio simulations.

The B3P combination of DFT functionals lead to an unrealistic force field and to some incorrect absorption intensities for α-pinene, while the BPW, P86 and B3L calculations provided qualitatively similar and correct representations of the vibrational absorption spectrum. This different accuracy of the functionals was not previously observed for calculation of electronic properties.

VCD spectroscopy not only can clearly distinguish between different chemical species but is also very sensitive to conformational changes in molecules. In borneol, this conformational dependence is amplified by the mechanical coupling of the C−O−H vibrations to the ring vibrational modes.

Acknowledgment. The work was supported by grants from the Grant Agency of the Czech Republic (203/95/0105) and (203/97/P002) and by a grant from Natural Sciences and Engineering Research Council of Canada.

References and Notes

(1) Tam, C. N.; Bouř, P.; Keiderling, T. A. *J. Am. Chem. Soc.* **1996**, *118*, 10285.

(2) Bouř, P.; Tam, C. N.; Shaharuzzaman, M.; Chickos, J. S.; Keiderling, T. A. *J. Phys. Chem.* **1996**, *100*, 15041.

(3) Bouř, P.; Keiderling, T. A. *J. Am. Chem. Soc.* **1993**, *115*, 9602.

(4) Maharaj, V.; Tsankov, D.; van de Sande, H. J.; Wieser, H. *J. Mol. Struct.* **1995**, *349*, 25.

(5) Devlin, F. J.; Stephens, P. J. *J. Am. Chem. Soc.* **1994**, *116*, 5003.

(6) Devlin, F. J.; Stephens, P. J.; Cheeseman, J. R.; Frisch, M. J. *J. Am. Chem. Soc*. **1996**, *118*, 6327.
(7) Yang, D.; Rauk, A. *J. Chem Phys.* **1992**, *97*, 6517.
(8) Stephens, P. J. *J. Phys. Chem.* **1985**, *89*, 748.
(9) Stephens, P. J. *J. Phys. Chem.* **1987**, *91*, 1712.
(10) Amos, R. D. CADPAC 5.0; SERC Laboratory: Daresbury, U.K., 1990.
(11) Bouř, P. *Chem. Phys. Lett.* ***1997***, *265*, 65.
(12) Freedman, T. B.; Spencer, K. M.; Ragunathan, N.; Nafie, L. A.; Moore, J. A.; Swab, H. M. *Can. J. Chem.* ***1991***, *69*, 1619.
(13) Bouř, P.; Baumruk, V.; Hanzliková, J.; *Collect. Czech. Chem. Commun*. in press.
(14) Tsankov, D.; Eggimann, T.; Wieser, H. *Appl. Spectrosc*. **1995**, *49*, 132.
(15) Becke, A. D. *J. Chem. Phys.* **1993**, *98*, 5648.
(16) Lee, C.; Yang, W.; Parr, R. G. *Phys. Rev. B* **1988**, *37*, 785.
(17) Frisch, M. J.; et al. *GAUSSIAN 94*; Gaussian Inc.: Pittsburgh, PA, 1994.
(18) De Proft, F.; Geerlings, P. *J. Chem. Phys.* **1997**, *106*, 3270.
(19) Perdew, J. P.; Wang, Y. *Phys. Rev. B* **1992**, *45*, 13244.
(20) Becke, A. D. *Phys. Rev. A* **1988**, *38*, 3098.
(21) Perdew, J. P. *Phys. Rev. B* **1986**, *33*, 8822.
(22) Labcalc, Galactic Industries Corp., 1992.
(23) Bouř, P.; Sopková, J.; Bednárová, L.; Malon, P.; Keiderling, T. A. *J. Comput. Chem.* **1997**, *18*, 646.
(24) Pulay, P. *J. Phys. Chem.* **1995**, *99*, 3093.
(25) Bouř, P; *J. Phys. Chem.* **1994**, *98*, 8862.
(26) Barron, L. D. *Molecular Light Scattering and Optical Activity*; Cambridge University Press: Cambridge, 1982.
(27) Devlin, F. J.; Stephens, P. J.; Cheeseman, J. R.; Frisch, M. J. *J. Am. Chem. Soc.* **1996**, *118*, 6327.